PII: S0032-3861(97)10177-X

Polymer Vol. 39 No. 21, pp. 5223–5239, 1998
0032-3861/98/$ – see front matter

Surface characterization of ethylene-vinyl acetate (EVA) and ethylene-acrylic acid (EAA) co-polymers using XPS and AFM

Ruth L. McEvoy‡, Sonja Krause* and Peter Wu†
Department of Chemistry and Polymer Science and Engineering Program, Rensselaer Polytechnic Institute, Troy, NY 12180-3590, USA
(Received 28 July 1997; accepted 30 September 1997)

The air surfaces of ethylene-vinyl acetate (EVA) co-polymers with 9–70 wt% vinyl acetate (VA) and ethylene-acrylic acid (EAA) co-polymers with 3–20 wt% acrylic acid (AA) were studied using XPS at three take-off angles, representing three depths of penetration from 15–58 Å. The semi-crystalline EVA and EAA co-polymers with high wt% ethylene (9–27.5 wt% VA) had higher percentages of VA at the surface than in the bulk, regardless of the type of sample preparation. Excess VA or AA at the surfaces of the annealed semi-crystalline films was probably the result of the rejection of VA or AA units from the growing crystallites. Spin and solution cast films generally had a greater percentage of VA at their surfaces than annealed films; this additional excess may be caused by the lower solubility of the ethylene units in the toluene used for casting, leaving a layer of the more soluble VA units on the air surfaces. Amorphous EVA co-polymer (50–70 wt% VA) annealed films showed an excess of ethylene at the surface. This occurred even though there are only very short sequences of ethylene in these co-polymers and was probably caused by the lower surface free energy of the ethylene repeat units with respect to the VA repeat units. The EAA co-polymers, all of which were semi-crystalline, always showed an excess of AA at the air surfaces, probably because of the rejection of the AA units by the crystallites. AFM bearing–ratio curves showed a fractional coverage of VA on 9EVA and 18EVA annealed surfaces of 0.885 and 0.927, respectively. When the XPS data were used with a simple model, which assumed a partial VA layer over a polyethylene layer at annealed co-polymer surfaces, a 2.0 Å layer of VA on the 9EVA and 18EVA surfaces, with surface coverages of 0.91 and 0.96, respectively, was calculated, in reasonable agreement with the AFM bearing–ratio data.

(Keywords: air surfaces; XPS; AFM)

INTRODUCTION

Surface segregation in phase-separated multi-component polymer blends and block and graft co-polymers has been studied extensively during the past 25 years[1–11 12–16]. In these studies, only a few of which have been cited, it was generally found that the lower surface free energy component migrated to the air surface during sample preparation. When the possibility of surface segregation in random co-polymers was studied[16,17], usually no surface segregation was found.

While the present work on ethylene-vinyl acetate (EVA) and ethylene-acrylic acid (EAA) random co-polymers was in progress, others[18–20] were studying the compositions of some of the same co-polymers after moulding against different substrates. Chihani *et al.*[18] studied EVA and EAA co-polymers moulded against perfluorinated ethylene propylene co-polymer (FEP), polytetrafluoroethylene, and poly(ethylene terephthalate) (PET). The resulting surfaces were studied using X-ray photoelectron spectroscopy (XPS) at a single take-off angle and by contact angle measurements. The XPS data on surface oxygen and carbon content indicated that EVA co-polymers containing from 9 to 28 wt% vinyl acetate (VA) had a slightly higher VA content at the surface than in the bulk polymer when moulded against FEP, and a slightly lower VA content at the surface than in the bulk when moulded against PET. The XPS data on EAA co-polymers containing from 3 to 20 wt% acrylic acid (AA), on the other hand, indicated a considerably higher AA content at the surface than in the bulk polymer when moulded against PET, and a considerably lower AA content at the surface than in the bulk when moulded against FEP; these differences were very small until the AA content of the co-polymer was at least 6.5 wt%. The EAA data were not surprising since the polar AA groups in the co-polymer were expected to migrate toward the polar PET surface during moulding while the non-polar ethylene groups were expected to migrate toward the FEP surface during moulding. The EVA data were somewhat puzzling. In a later study[20], XPS data were obtained at two different take-off angles, corresponding to two different penetration depths, and some of the co-polymer surfaces were annealed against air after moulding against a PET film. Now the EVA co-polymers showed a VA content at the surface, using both take-off angles, that was greater than the bulk value whether the samples were moulded against FEP or PET. The EAA co-polymers that were moulded against FEP had decreased AA contents, compared to the bulk values, at both take-off angles. The EAA co-polymers that were moulded against PET, however, had AA contents that were lower than the bulk values at a 10° take-off angle (this is the outermost

* To whom correspondence should be addressed
‡ Present address: Schenectady Community College, Washington Ave., Schenectady, NY 12305, USA.
† Present address: Department of Physics, Southern Oregon University, 1250 Siskiyou Blvd., Ashland, OR 97520, USA.

layer) and higher than the bulk values at a 38.5° take-off angle (this includes some polymer repeat groups below the outermost layer). The oxygen contents of the outermost layers were about the same, for all EAA co-polymers, whether they were moulded against FEP or PET. It was the AA content just below this layer that was very different, depending on the mould material. Co-polymer films that were annealed in air were examined using contact angles of water and methylene iodide and were compared with those measured on the original surfaces, as moulded against PET. The EAA surfaces apparently restructured and became more hydrophobic during annealing, the contact angles becoming the same within experimental error. The EVA surfaces did not change noticeably during annealing.

Galuska[19] used XPS and time-of-flight secondary ion mass spectroscopy (ToF-SIMS) to study the air surfaces of EVA co-polymers containing from 3.0 to 29.2 wt% VA. He concluded that there was a thin (≤ 20 Å thick) VA-enriched layer directly at the air surface, with an ethylene-rich layer just below it in all samples, whether these were spin coated, pressed or extruded.

The purpose of the present work was to study the composition at the air surface of a wide variety of EVA and EAA films after spin casting, solvent casting and annealing, and to understand the results, if possible. XPS was used on all samples at three take-off angles and atomic force microscopy (AFM) was used to study a few of the samples. The sequence distributions of many of the co-polymers were studied using high resolution ^{13}C nuclear magnetic resonance (n.m.r.).

EXPERIMENTAL

Materials

Table 1 shows the source and molecular weight of all the commercial polymer samples studied in this work. Molecular weights, when shown, were determined by gel permeation chromatography (g.p.c.) or provided by the supplier. Samples were used as received.

Differential scanning calorimetry (d.s.c.)

All the samples were studied using a Perkin Elmer DSC7 Differential Scanning Calorimeter interfaced with a Nec Multisync II computer. The samples were cut with a clean razor blade directly from the co-polymer pellets as received from the supplier. All thermograms were obtained at a heating rate of 10°C per min. Nitrogen was used as the purge gas in the glove box. Thermal analysis software used for processing the data was present on the hard drive of the computer. The percentage crystallinity was calculated, from a second heating cycle, by dividing the heat of fusion of each co-polymer per gram of ethylene in the d.s.c. sample pan by the heat of fusion of linear polyethylene between 350 and 450 K[21], 293 J g^{-1} and multiplying by 100.

Nuclear magnetic resonance (n.m.r.)

^{13}C n.m.r. spectra of co-polymers containing ≥ 27.5 wt% VA in EVA were obtained using a 200 MHz Varian XL-200 Fourier-Transform (FT) n.m.r. spectrometer. Samples were prepared in deuterated chloroform and tetramethylsilane was used as an internal reference. ^{13}C n.m.r. spectra of 9EVA and 18EVA were obtained in deuterated *p*-xylene solution using a 500 MHz Unity 500/51 n.m.r. spectrometer. The 9EVA was heated to 100°C and the 18EVA was heated to 85°C while the data were obtained.

Preparation of co-polymer samples for XPS and scanning electron microscopy (SEM)

Samples were prepared in four ways: spin cast, solution cast, spin cast annealed and melt pressed annealed. Pure EVA samples were both spin cast and solution cast from 4% w/v solutions in toluene on to silicon wafers. Melt pressed samples of 9EVA, 14EVA, 18EVA and all EAA co-polymers were prepared by placing one pellet of the co-polymer on a silicon wafer, heating above the melting temperature, then pressing the melted pellet down using a glass slide. Crystalline samples were annealed at approximately 20°C above their melting temperatures for 72 hours while amorphous samples were annealed for 72 hours at 60°C in a vacuum oven. *Table 2* shows the melting points, percentage crystallinity and annealing temperatures for all the co-polymer films.

X-ray photoelectron spectroscopy (XPS)

X-ray photoelectron spectroscopy analysis was performed on a Perkin Elmer model 1257 ESCA spectrometer which was interfaced with a Domain 3000 computer; Perkin Elmer software was used for processing data. Data analysis was performed on unsmoothed curves. The instrument uses a monochromatic Mg anode which was operated at 15 kV and 200 W and the pressure in the source chamber was approximately 10^{-9} torr. The analysis spot size was 1 × 1 mm. The samples were neutralized by flooding with electrons during analysis. They were all analysed at three

Table 1 Polymers used in this work

Designation	Composition	Source	$M_w \times 10^{-4}$
9EVA	9 wt% VA	SPP[a]	NA[b]
14EVA	14 wt% VA	SPP[a]	NA[b]
18EVA	18 wt% VA	SPP[a]	NA[b]
27.5EVA	27.5 wt% VA	Exxon	1.01
40EVA	40 wt% VA	SPP[a]	7.3
45EVA	45 wt% VA	SPP[a]	19.7
50EVA	50 wt% VA	SPP[a]	16.2
70EVA	70 wt% VA	SPP[a]	16.0
3EAA	3 wt% AA	Dow	8.57
6.5EAA	6.5 wt% AA	Dow	7.91
9.7EAA	9.7 wt% AA	Dow	19.4
20EAA	20 wt% AA	Dow	7.68
HDPE	High density polyethylene	Phillips	12.3
PVA	Poly (vinyl acetate)	Hoechst	NA[b]
PAA	Poly (acrylic acid)	SPP[a]	0.20

[a]Scientific Polymer Products.
[b]Not available.

Table 2 Melting temperatures, % crystallinity, and annealing

Temperatures of the co-polymers				
Sample	$\|T_m\|$		% Crystallinity	Annealing T (°C)
	°C	K		
9EVA	93	366	19	112
14EVA	91	364	17	112
18EVA	83	356	11	105
27.5EVA	75	348	8	90
40EVA	49	322	~1	65
45EVA	None[a]		0	60
50EVA	None		0	60
70EVA	None		0	60
3EAA	108	381	24	130
6.5EAA	103	376	17	130
9.7EAA	97	370	17	130
20EAA	96	369	9	120

[a]A small melting peak appeared at 43°C on first melting which indicated less than 1% crystallinity. This peak disappeared on remelting after cooling.

angles relative to the sample surface: 15°, 45° and 75°, corresponding to maximum sampling depths of approximately 15, 42 and 58 Å, respecively[22,23].

Scanning electron microscopy (SEM)

A Zeiss CSM 950 scanning electron microscope was used to study the air surfaces of the EVA and EAA films. The films were prepared on silicon wafers, then the wafers were pressed against carbon tape and mounted on aluminium stubs. A thin layer of gold was deposited on all samples using a Denton Desk II sputter coater with a gold target. Coated samples were observed and photographs were taken using a Polaroid instant camera.

Atomic force microscopy (AFM)

Films of 9EVA, 18EVA, HDPE and PVA were melt pressed on to silicon wafers as in the preparation of samples for XPS. 9EVA, 18EVA and HDPE were annealed for 72 hours at 20°C above their melting temperatures while PVA was annealed for 72 hours at 60°C. The sample surfaces were scanned under ambient conditions using a Topometrix Model TMX 2000 employing either a modulated or a non-modulated cantilever. For modulated modes, the base of the cantilever was mounted on a piezoelectric ceramic which is used as an oscillator.

Three different imaging modes were used to move the AFM probe over the sample surface. (1) Topography or DC (contact) mode which results in a plot of the height of surface features as a result of vertical deflection of the cantilever. (2) Lateral Force Microscopy (contact-friction) is a modification of the topographic image and results in a plot of torsional motions of the cantilever arising from frictional interactions between the sample surface and the probe tip. (3) Force Modulation Spectroscopy (contact-compliance, i.e. 'hardness') mode results in a plot of regions of differing sample compliance as a result of differential cantilever deflection in response to a small amplitude modulation of the tip. In this mode the cantilever oscillated at a frequency of 5 kHz and an amplitude of 5–15 Å. Bearing–ratio (B–R) calculations were also performed on the modulated force images. B–R curves represent the percentage of materials in the sample of differing 'hardness.' Domains of sharply differing 'hardness' produce steps or kinks in the B–R curve.

RESULTS AND DISCUSSION

Sequence distributions in the EVA co-polymers

The integrated areas under the peaks in the methylene and methine regions of the ^{13}C NMR spectra were used to determine the percentages of various repeat unit triad structures as in the work of Wu *et al.*[24]. *Table 3* shows the locations of the peaks observed in that work and in the present work and the monomer triads responsible for each peak. *Table 4* shows the percentage of the different types of repeat groups found in each co-polymer in this work. Since only the vinyl acetate repeat group contains a methine carbon, the methine region data can be used by themselves both to determine whether they are consistent with Bernouillian statistics for monomer addition during polymerization and to calculate the number average sequence length of the vinyl acetate repeat groups in the co-polymers

Table 3 The ^{13}C NMR peaks from the methylene and methine regions of the spectra in the EVA co-polymers measured in deuterated chloroform. The peaks have been attributed to the central repeat unit of the triads shown in the table by Wu *et al.*[24]. In the triads, E stands for an ethylene repeat unit and V stands for a vinyl acetate repeat unit

Triad	Methine region	
	From [24] (ppm)	This work (ppm)
VVV	65.6	66.9 and 69.7
EVE	70.1	Doublet at 70.0, plus peaks at 70.9 and 71.2
EVV	74.6	Triplet at 74.5
	Methylene region	
VVV and VVE	38.8 and 39.4	38.8 and 39.4
EEV, EVE, VEV, and VEE	34.3 and 34.5	34.3 and 34.5
EEV and EEE	29.6	29.6
VEE and EEV	25.4	25.4
EVE[a]	21.1	21.1

[a]This peak includes a contribution from the methyl group in vinyl acetate and was not used in further calculations.

Table 4 Percentage of different triads in the EVA co-polymers calculated from the ^{13}C NMR spectra. Both the triads absorbing in the methine region of the spectrum and those absorbing in the methylene region have been calculated separately on the basis of 100% each

Polymer	Methine region			Methylene region			
	%EVE	%VVE	%VVV	%VVV + VVE	%EVE + VEV + 2VEE[a]	%EEV + EEE	% 2VEE[a]
9EVA	100	0	0	0.01	1	93	6
18EVA	100	0	0	0.08	11	83	15
27.5EVA	75	24	1	1	13	76	10
33EVA	72	27	1	2	16	70	11
40EVA	67	30	3	2	19	65	14
45EVA	57	37	6	3	20	61	15
70EVA	32	44	24	16	34	33	17

[a]2VEE refers to the VEE plus the EEV peak.

Table 5 Number average sequence lengths of vinyl acetate and ethylene in the EVA co-polymers determined from ^{13}C NMR and Bernouillian statistics

Polymer	Vinyl acetate	Ethylene
9EVA	1.0	32.4
14EVA	1.0	19.9
18EVA	1.1	15.1
27.5EVA	1.2[a]	9.1
33EVA	1.2[a]	7.3
40EVA	1.2[a]	5.6
45EVA	1.3[a]	4.8
70EVA	1.9[a]	2.4

[a]From ^{13}C NMR data. All others were calculated assuming Bernouillian statistics for the addition of monomer during co-polymerization.

containing $\geq$ 27.5 wt% VA. The data from the methylene region come from both the ethylene and the vinyl acetate repeat groups; they can be used to determine whether they are consistent with Bernouillian statistics, but cannot be disentangled to provide the sequence lengths of the ethylene and vinyl acetate repeat groups in the co-polymers. Thus, the data in *Table 4* agree with Bernouillian statistics for monomer addition but only the methine region data could be used calculate the number average sequence length of some of the VA units in some of the co-polymers[25]. The number average sequence length of the VA units in the other co-polymers and the ethylene units in all the co-polymers were calculated assuming Bernouillian statistics for monomer addition during co-polymerization; Wu *et al.*[24] had previously found that the co-polymerization of their EVA co-polymers followed Bernouillian statistics. The calculated sequence lengths of ethylene and VA are shown in *Table 5*.

SEM of the co-polymer surfaces

EVA. The surfaces of the EVA co-polymers had differing topographies which varied depending on the method of preparation. *Figure 1* shows that 9EVA melt pressed and annealed films had surface structures that looked like spherulites that had grown together; these spherulites appeared to have fibrils radiating from their centres. Surfaces of solution cast 9EVA films, however, as shown in *Figure 2*, appeared to consist of thick fibres with no definite spherulitic structures; spin cast films of 9EVA appeared similar to the solution cast films. Pressed and annealed films of 14EVA showed structures that resembled the spherulites seen on the surface of the pressed and annealed 9EVA film (*Figure 1*) but these were smaller. *Figure 3* shows the surface of a spin cast film of 14EVA; the solution cast film had

Figure 2 SEM micrograph of 9EVA air surface: solution cast film

Figure 3 SEM micrograph of 14EVA air surface: spin cast film

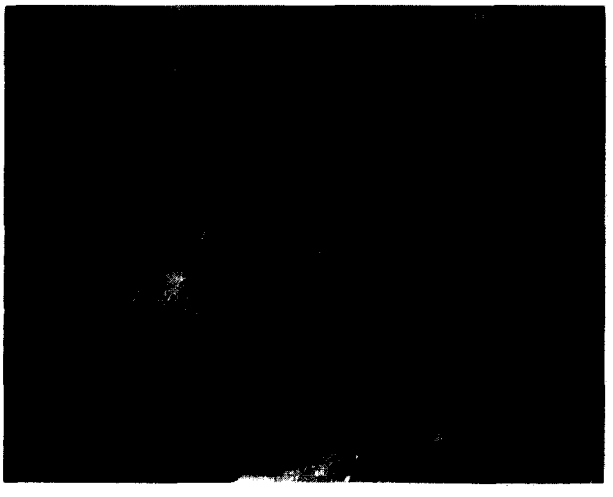

Figure 1 SEM micrograph of 9EVA air surface: pressed and annealed film

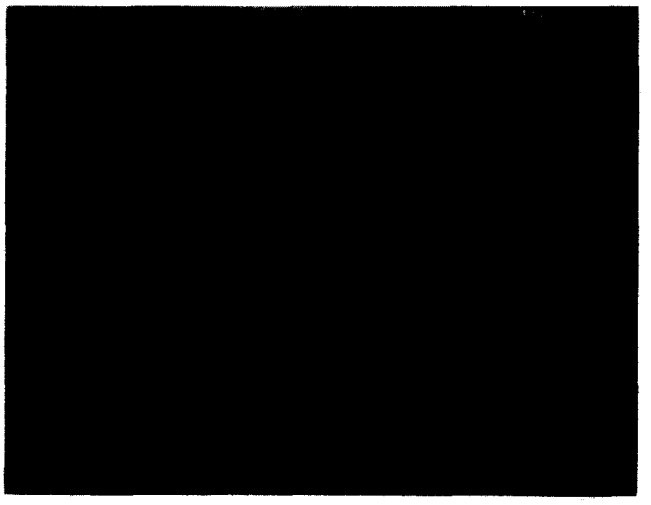

Figure 4 SEM micrograph of 3EAA air surface: pressed and annealed film

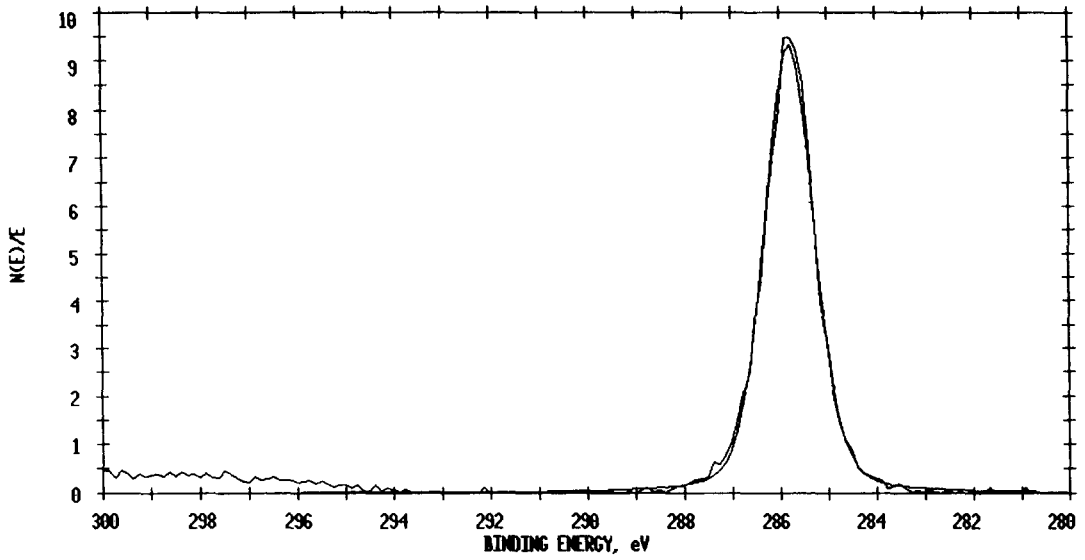

Figure 5 XPS core binding energies for HDPE

a similar appearance. The air surface of pressed and annealed 18EVA films showed even smaller spherulitic structures than the 14EVA, again with radiating fibrils. The spin cast film of 18EVA appeared somewhat lumpy but was essentially featureless; the solution cast film appeared virtually flat. All EVA films containing > 18 wt% VA looked flat in the SEM.

EAA. All EAA film surfaces showed faint structures that appeared somewhat spherulitic. *Figure 4* shows the air surface of a pressed and annealed film of 3EAA which showed the most pronounced structures of all the EAA films. The spherulite-like structures decreased in size as the percentage AA increased in the co-polymers.

XPS of co-polymer surfaces

Quantification of the VA or AA content of the surfaces was accomplished by resolving the component peaks in the C(1s) signal. Pure polyethylene, PAA and PVA were first analysed to determine the positions of the component peaks in the C(1s) signal. The characteristic XPS core level binding energy for polyethylene, which has a defined peak at a binding energy of 285.0 eV, as well as for PVA and PAA are shown in *Table 6*.

Table 6 Characteristic XPS core level binding energies for polyethylene, PVA, and PAA

Polymer	Peak	Binding energy (eV)
Polyethylene	CH_x	285.0
PVA	CH_x	285.0
	CC=OR	285.5
	COC=O	286.6
	C=OO	289.2
PAA	CH_x	285.0
	CC=OR	286.2
	C=OO	289.2

Figures 5–7 show binding energy curves for pure polyethylene, PVA and PAA at a 45° angle. *Figures 8–11* show binding energy curves for 9EVA, 45EVA, 70EVA and 3EAA at all angles. The resolution into the component peaks is shown in each case.

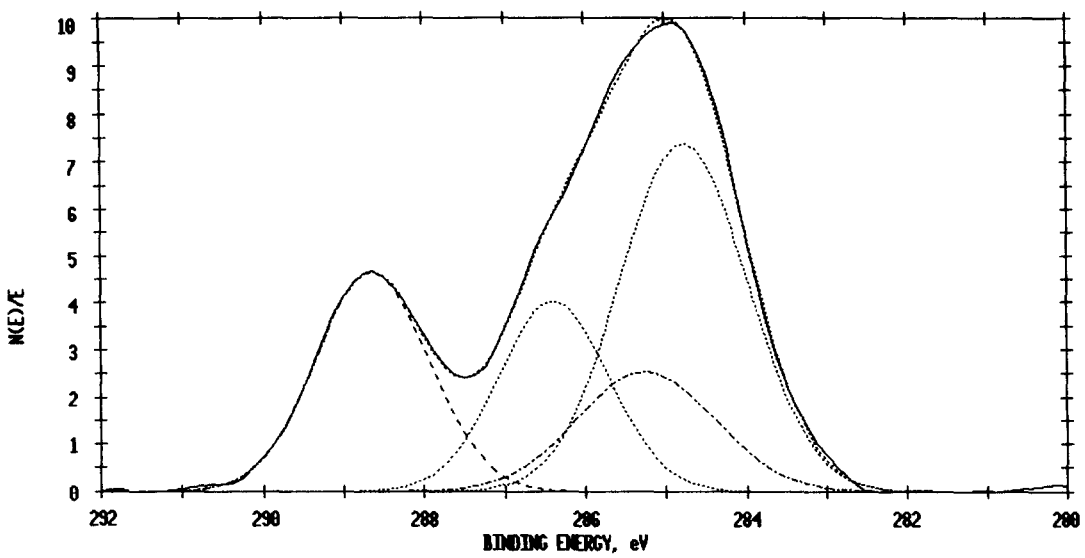

Figure 6 XPS core binding energies for PVA

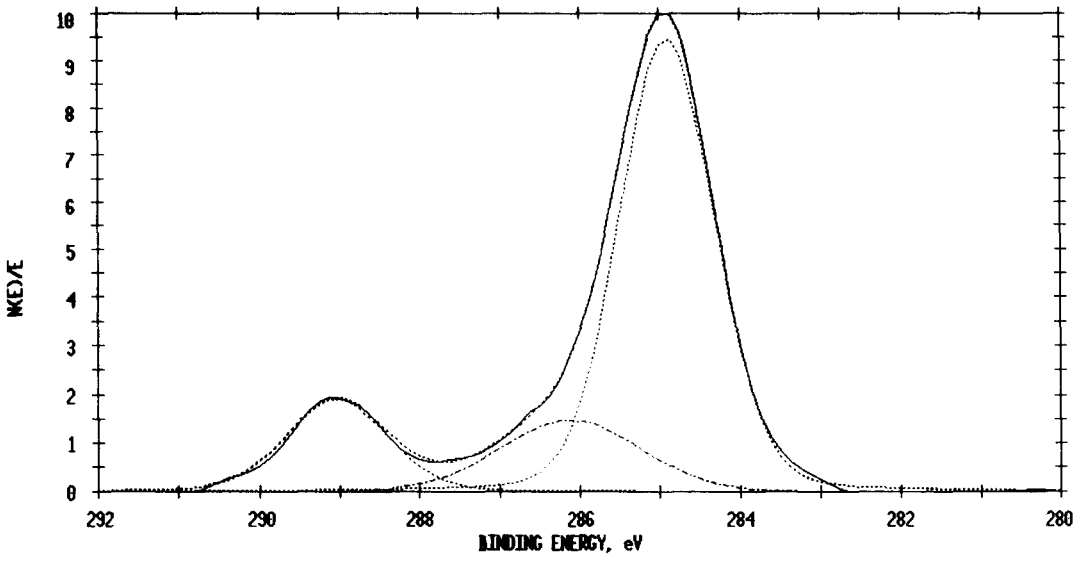

Figure 7 XPS core binding energies for PAA

The percentage VA or AA was calculated using the *C*=OO carbon peak intensity relative to all other carbon peaks. To determine the percentage VA from the XPS data, it was assumed that all carbons in the different chemical environments had the same sensitivity factor[26]. The intensity of each carbon peak from the XPS C(1s) spectra was given a value equal to the number of moles of the group responsible for that peak in 100 g of analysed sample, as follows:

$$I_{C\text{-}OO} = w_{VA}/86 \quad (1)$$

$$I_{COC=O} = w_{VA}/86 \quad (2)$$

$$I_{CH} = 2w_{VA}/86 + 2(1 - w_{VA})/28 \quad (3)$$

where w_{VA} is the wt% VA in the sample, 86 is the molecular weight of the VA repeat group, and 28 is the molecular weight of the ethylene repeat group. Since only carbon peaks were investigated, the sum $I_{C\text{-}OO} + I_{COC=O} + I_{CH}$ equals 100. Using this information and equations (1)–(3), one may solve for w_{VA}:

$$w_{VA} = (0.0714I_{C=OO})/(1.16 + 0.025I_{C=OO}) \quad (4)$$

In the same way, the expression for obtaining the wt% AA at the surface, w_{AA}, becomes:

$$w_{AA} = (0.0714I_{C=OO})/(1.39 + 0.0297I_{C=OO}) \quad (5)$$

Table 7 shows the percentage VA or AA calculated at various penetration depths in all the co-polymers investigated.

EVA co-polymers. *Table 7* shows that the 45EVA, 50EVA and 70EVA samples, which were ≤ 1% crystalline (*Table 2*), had less than the bulk percentage of VA at and near their air surfaces, except for the cast samples of 45EVA and 50EVA at 15 Å penetration. This means that there was an excess of ethylene at and near the surfaces of most of these films even though the calculated number average ethylene sequence lengths of these co-polymers varied only between 2 and 6 (*Table 5*). Thus, even the very short sequences of ethylene appear to move preferentially to the surface in these amorphous samples, probably because homo-polymers of ethylene such as HDPE and low density polyethylene (LDPE) have lower surface free energies (surface tensions) than PVA (see *Table 8*), at least near

Table 7 Percentage VA or AA in spin cast, solution cast and annealed films of EVA and EAA surfaces at various penetrations from XPS analysis

Sample	Spin cast			Solution cast			Melt pressed and annealed		
	Maximum sampling depth			Maximum sampling depth			Maximum sampling depth		
	15 Å	42 Å	58 Å	15 Å	42 Å	58 Å	15 Å	42 Å	58 Å
9EVA	46	17	7	64	15	10	39	7	4
14EVA	58	28	19	54	32	24	39	13	14
18EVA	61	38	39	60	11	12	41	13	14
27.5EVA	52	38	33	NA	NA	NA	71	22	26
40EVA	55	46	41	NA	NA	NA	46	45	45
45EVA	46	39	38	49	38	38	41	37	38
50EVA	57	35	31	NA	NA	NA	28	28	32
70EVA	49	55	58	48	58	58	38	60	60
3EAA	NA	NA	NA	NA	NA	NA	35	5	6
6.5EAA	NA	NA	NA	NA	NA	NA	35	8	8
9.7EAA	NA	NA	NA	NA	NA	NA	22	8	6
20EAA	NA	NA	NA	NA	NA	NA	53	7	6

NA indicates data not available.

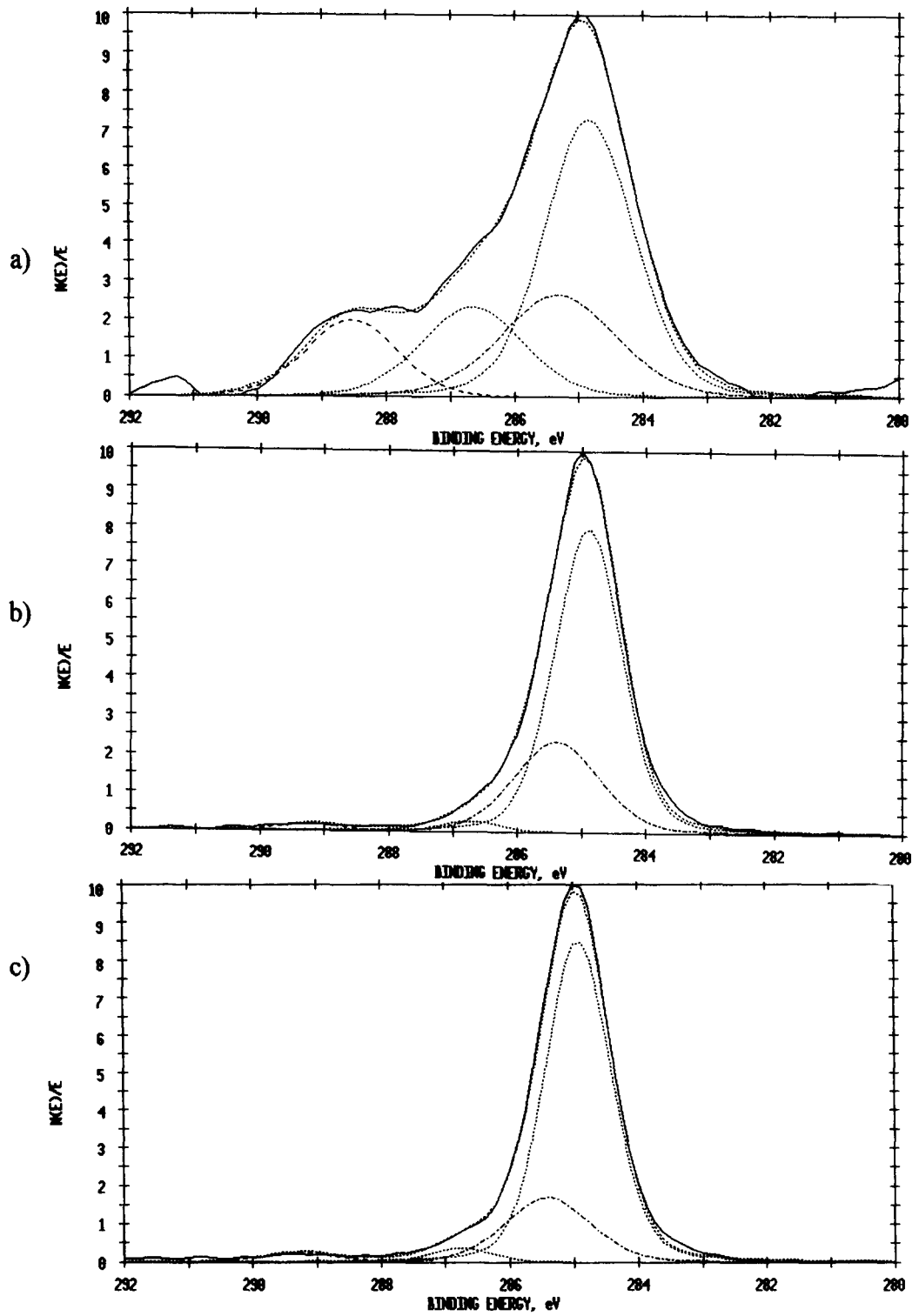

Figure 8 XPS binding energies of annealed 9EVA air surface at (a) 15°, (b) 45°and (c) 75°

room temperature. (The annealing temperature of these amorphous samples was 60°C, closer to room temperature than the higher temperatures shown in *Table 8*, where the situation appears reversed, at least with respect to HDPE and PVA.) At deeper penetrations than 15 Å, the weight percentage VA approaches the bulk values (*Table 7*). The only exception to the general behaviour of the amorphous co-polymers appears to be the 50EVA spin cast films, which had somewhat greater weight percentage VA than that of the bulk VA at 15 Å penetration. Since all the films were cast from toluene, in which PVA is soluble at room temperature and in which polyethylene is not, there could have been some surface enrichment in VA due to its higher solubility. In fact, *Table 7* shows that all the cast amorphous EVA films had a higher surface VA content than the annealed film of the same co-polymer. Other workers have found that when the casting solvent for a di-, tri- or multiblock co-polymer was more preferential for one repeat unit, the segregation of that repeat unit to the surface increased[27–30].

All the EVA semi-crystalline samples (9EVA to 40EVA) showed an enhanced VA content at the air surface

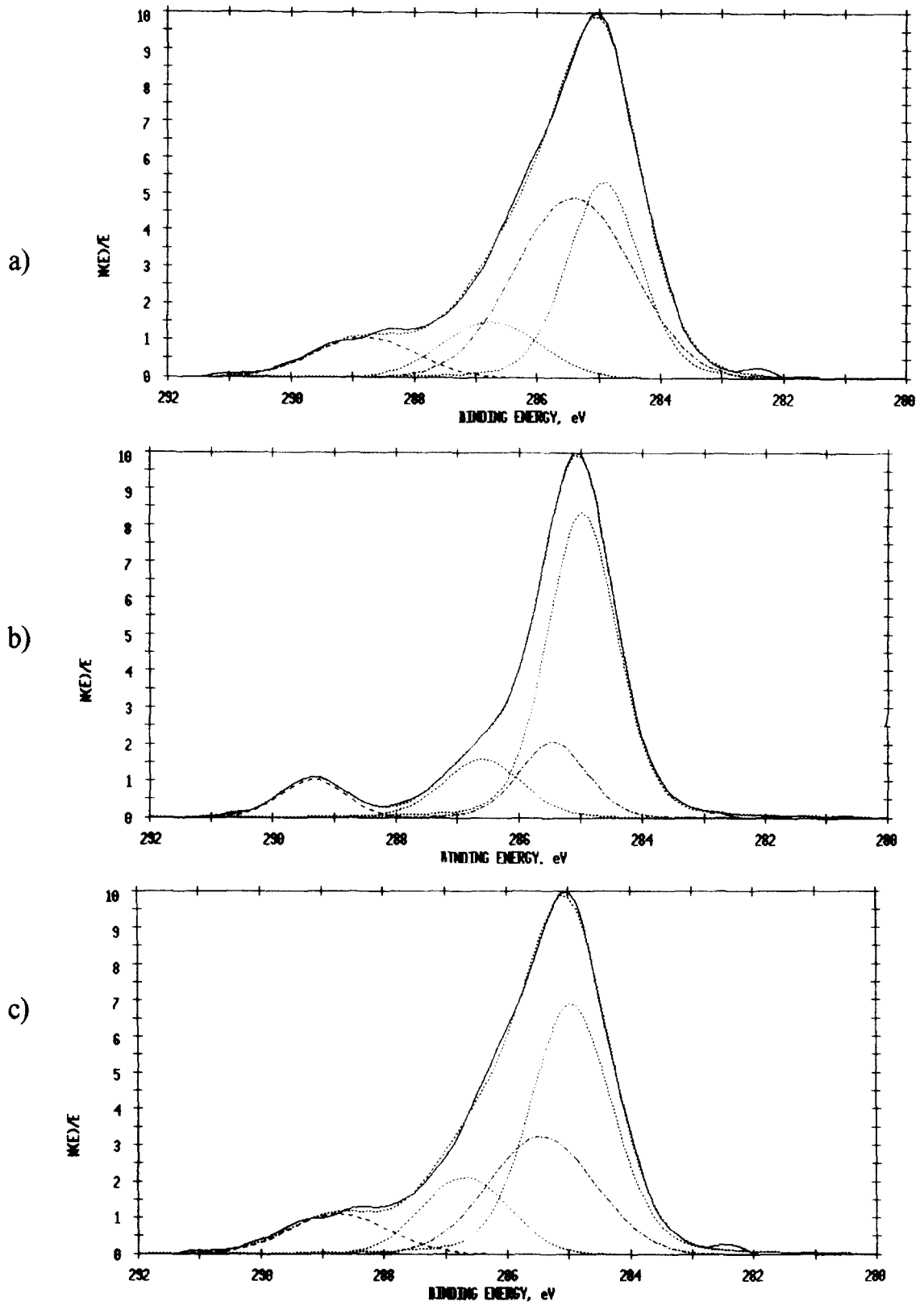

Figure 9 XPS binding energies of annealed 45EVA air surface at (a) 15°, b) 45° and (c) 75°

regardless of the manner in which the sample was prepared. Except in the cast of 27.5EVA, the percentage VA was greater at the surface for spin and solution cast films than for annealed films, again indicating surface enrichment of VA units due to their greater solubility in toluene. 27.5EVA was the only co-polymer examined in this work that contains anti-oxidants that may have diffused to the surface during annealing. Any carbon and oxygen containing anti-oxidants could masquerade as VA in these experiments. The VA enrichments at the surfaces of the semi-crystalline films occurred in spite of the fact that PVA has a higher surface tension at 20°C than LDPE and HDPE and may have a slightly lower surface tension at elevated temperatures depending on whether the sample is compared to HDPE or LDPE (*Table 8*). Also, the number average sequence length of VA in these co-polymers was never greater than two

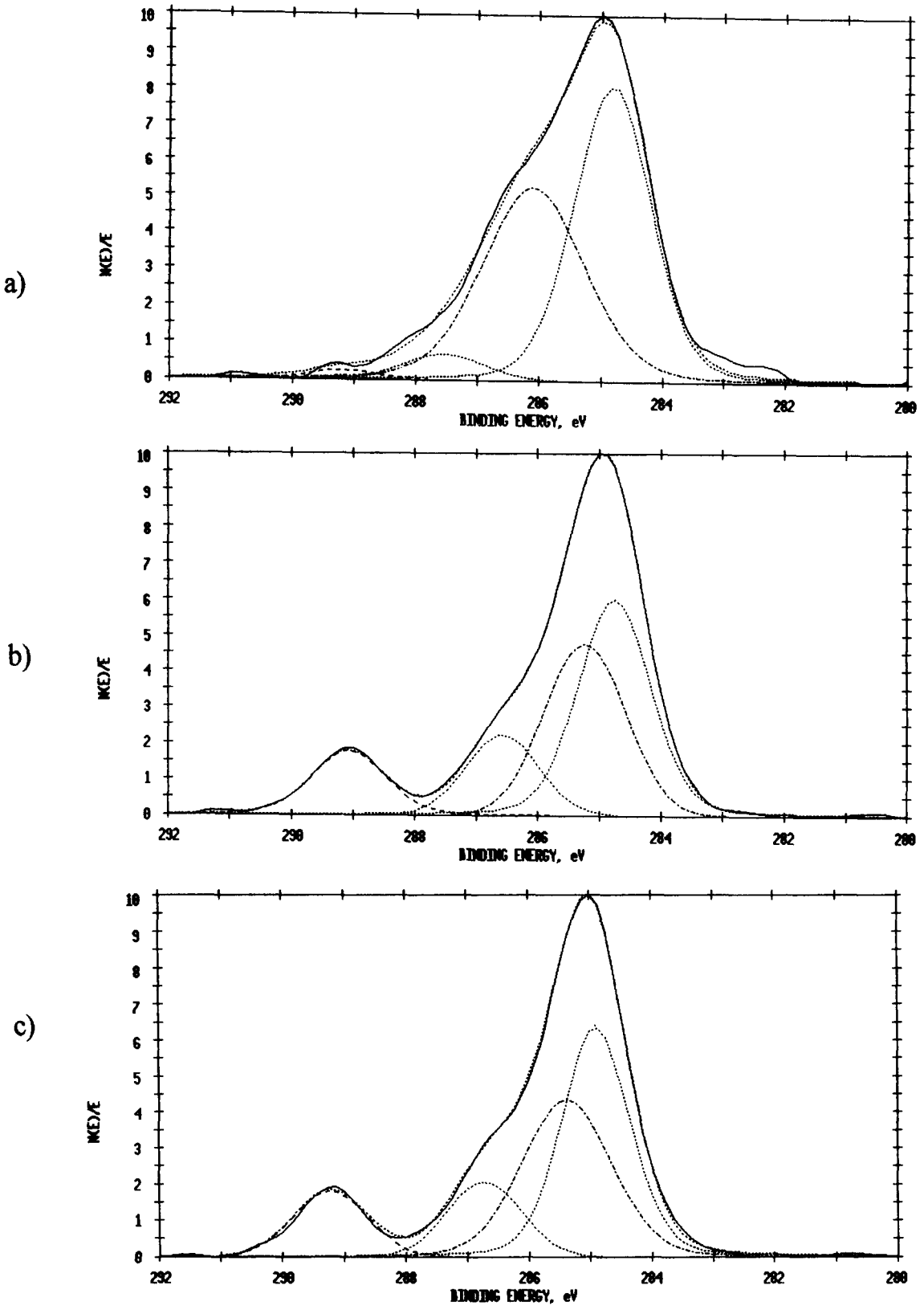

Figure 10 XPS binding energies of annealed 70EVA air surface at (a) 15°, (b) 45° and (c) 75°

units according to ^{13}C n.m.r. data (*Table 3*). In these semi-crystalline samples, therefore, it is possible to postulate that the higher surface free energy VA sequences were rejected from the growing crystallites and forced to the surface of the film during crystallization of the co-polymer. Alamo *et al.*[31] and Domszy *et al.*[32] have also reported that a layer of the amorphous co-unit formed over polyethylene crystallites during crystallization of hydrogenated polybutadiene. Galuska[19] also found an excess of VA co-units at the immediate air surface in his studies of EVA co-polymers containing up to 29.2 wt% EVA, thus in the semi-crystalline range.

The 9EVA to 27.5EVA annealed, therefore closer to equilibrium, samples showed a wt% of VA greater than the

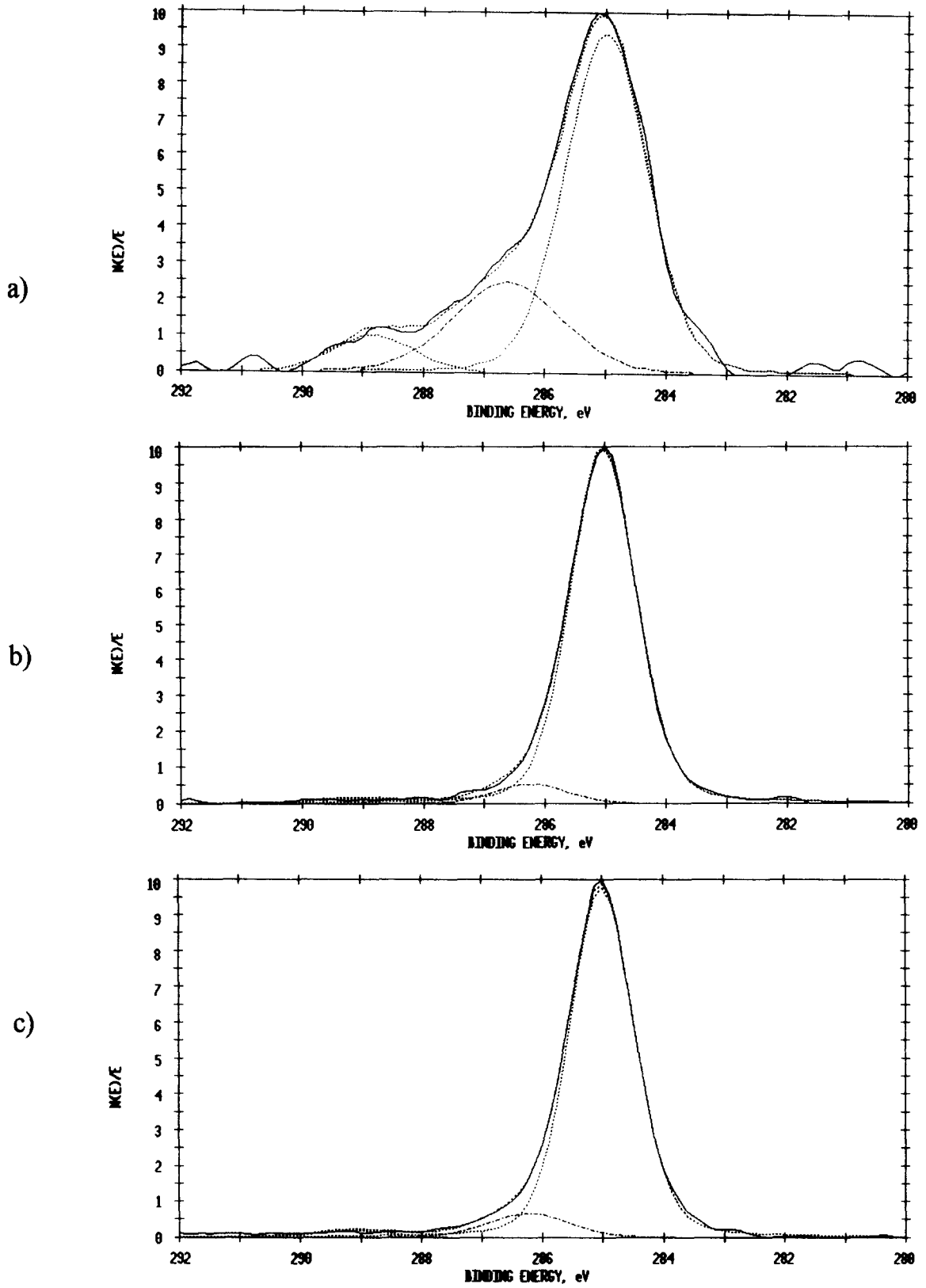

Figure 11 XPS binding energies of annealed 3EAA air surface at (a) 15°, (b) 45° and (c) 75°

bulk value at 15 Å lower than the bulk value at 42 and 58 Å penetration (*Table 7*). Thus, it appears that there may be an ethylene-enriched layer below the VA-enriched layer at these air surfaces when equilibrium is reached; below this, the bulk composition can be seen. Galuska[19] found similar results studying EVA co-polymers using XPS and time of flight SIMS.

XPS of EAA co-polymers

Table 7 also shows all the XPS-derived data of all the EAA co-polymers examined in this work. One may observe that there was an increase in the higher surface free energy component, AA, at the air surface of all EAA-annealed films. This occurred in spite of the much larger surface tension of PAA *versus* polyethylene. We may also note that

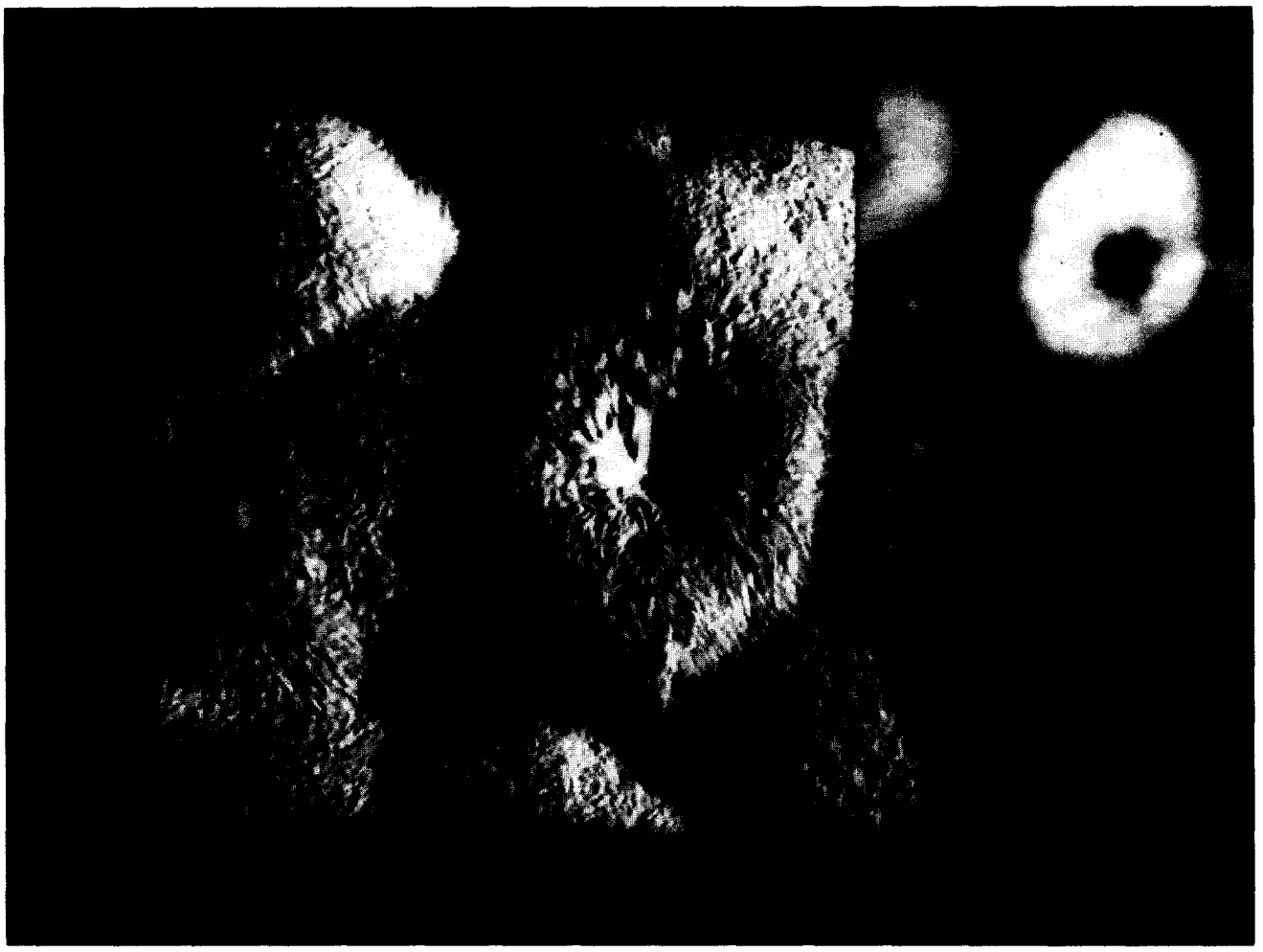

Figure 12 9EVA annealed surface AFM topographic image (2500 × 2500 nm)

all EAA samples were semi-crystalline, as shown in *Table 2*. Thus, as in the case of the semi-crystalline EVA samples, rejection of the AA segments from the crystallites to the air surface is a likely explanation.

AFM data

AFM topography mode images (*Figures 12 and 13*) of 9EVA and 18EVA annealed film surfaces show spherulite-like topography similar to that observed using SEM. Also, as shown by the SEM data, the spherulites of 18EVA appear smaller than those of 9EVA. An AFM-enhanced image of 9EVA (not shown), though somewhat blurred, revealed aligned fine fibres, averaging 75 nm in length, in the spherulitic structures.

AFM-modulated force images of HDPE and PVA (*Figures 14 and 15*) show samples that are relatively uniform, but quite different, in hue and therefore, in 'hardness' on the sample surfaces. The entire surface of HDPE is relatively 'lighter' and therefore 'softer' than the 'darker' PVA surface which is harder. In polymeric system, 'hardness' cannot always be defined as a measure of crystallinity because the amorphous material may be glassy or rubbery. Ordinarily, hardness is expressed using a number which is measured by a simple indentation test involving the application of a force to a vertical indentor using a calibrated spring. The Shore hardness scale, for example, is such a test in which a reading of 100 corresponds to pressing the indentor on to a sheet of plate glass while a reading of zero corresponds to the indentor meeting no resistance. Hardness tests by ASTM methods show that PVA has a hardness of 80–85 Shore units[33], LDPE has a hardness of 44–45 Shore units[34] and HDPE has a hardness of 55–70 Shore units[34] near room temperature. Thus, the modulated force results appear completely

Table 8 Surface tensions of HDPE, LDPE, PVA and PAA at 20°C, 140°C and 180°C[37]

Polymer	Surface tension (dyne/cm)		
	20°C	140°C	180°C
High density polyethylene (M_w = 6700)	35.7	28.8	26.5
Low density polyethylene (M_w = 7000)	35.3	27.3	24.6
Low density polyethylene (M_n = 2000)	33.7	26.5	24.1
Poly (vinyl acetate) (M_w = 11 000)	36.5	28.6	25.9
Poly (acrylic acid)	38.1[38]	34.9 (105°C)[34]	

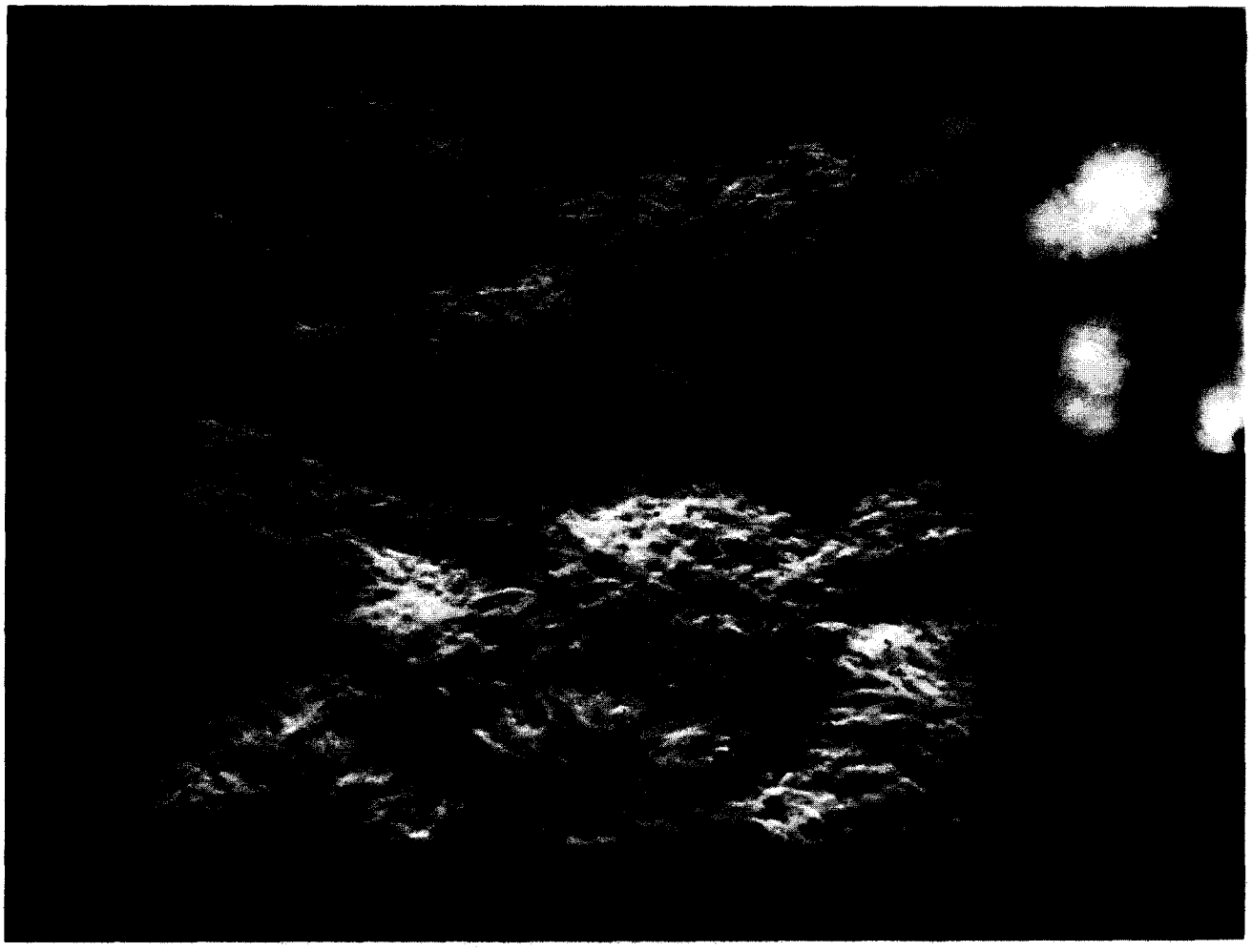

Figure 13 18EVA annealed surface AFM topographic image (2500 × 2500 nm)

reasonable, HDPE being softer than PVA. A substantial portion of the 9EVA and 18EVA sample surfaces are 'hard', corresponding to PVA, as seen in the modulated force images (not shown). It is possible to compute the percentage surface area corresponding to 'soft' and 'hard' areas with the application of bearing–ratio curves (*Figures 16 and 17*). These figures show that 88.5% of the surface is composed of 'harder' areas for 9EVA and 92.7% for 18EVA. Assuming that the 'harder' areas correspond to areas of VA, these surface areas correspond to the fraction of VA on the surfaces.

A simplified quantitative model to fit the XPS and AFM data

In order to quantify the XPS data in such a way as to calculate actual surface coverage with one of the two polymer repeat groups in a particular co-polymer, it is necessary to make a model. In the case of the semi-crystalline annealed co-polymers, especially 9EVA, 14EVA, 18EVA and all the EAA co-polymers, which exhibited enhanced VA or AA at 15 Å penetration, and a depletion of VA or AA at 42 and 58 Å penetration (except for 3EAA and 6.5EAA which had close to the bulk concentration of AA units below 15 Å penetration), the model consists of a fractional overlayer composed of VA or AA with thickness, d, which is less than the maximum penetration depth (56 Å) in our XPS experiments, over a thin substrate of ethylene, followed by the bulk content EVA or EAA (*Figure 18a*). The predicted intensity of the C(1s) signal for the C=OO peak using this model would be[35]:

$$I_0 = xI_0^{\infty}[1 - e^{-d/\lambda \cos\theta}] \quad (6)$$

where I_0 is the intensity of the overlayer signal (C=OO), I_0^{∞} is the intensity of the C=OO peak if the overlayer is made up of pure PVA or pure PAA, d is the thickness of the overlayer, λ is the inelastic mean free path of the electrons (~20 Å, as shown for electrons of ~1000 eV in poly-(*p*-xylylene) by Clark and Thomas[36]), θ is the angle of the electrons to the analyser from the surface, and x is the fraction of VA or AA in the overlayer. Ethylene is the substrate, and is assumed to occupy a depth down past 58 Å, the maximum sampling depth, and thus does not contribute to the intensity of the C=OO signal. This model allows for both ethylene and VA or AA at the air surface. Equation (1) contains two unknowns, x and d, thus giving a continuum of solutions. Different values of d give different values of x. A reasonable value of d was first calculated from the 15 Å penetration data assuming $x = 1$; these values did not agree with experimental data at higher penetrations. The value of x could then be calculated from this d and from the experimental data at higher penetration. The best values for the annealed samples of 9EVA, 14EVA and 18EVA were $d = 2$ Å and $x = 0.91$, 0.92 and 0.96, respectively. Considering the very simple model used, the values calculated for 9EVA and 18EVA are in excellent agreement with those from the AFM bearing–ratio curves, 0.885 and 0.927 for 9EVA and 18EVA, respectively. In the case of the EAA films, $d = 1.5$ Å for 3EAA, 6.5EAA and 9.7EAA, with

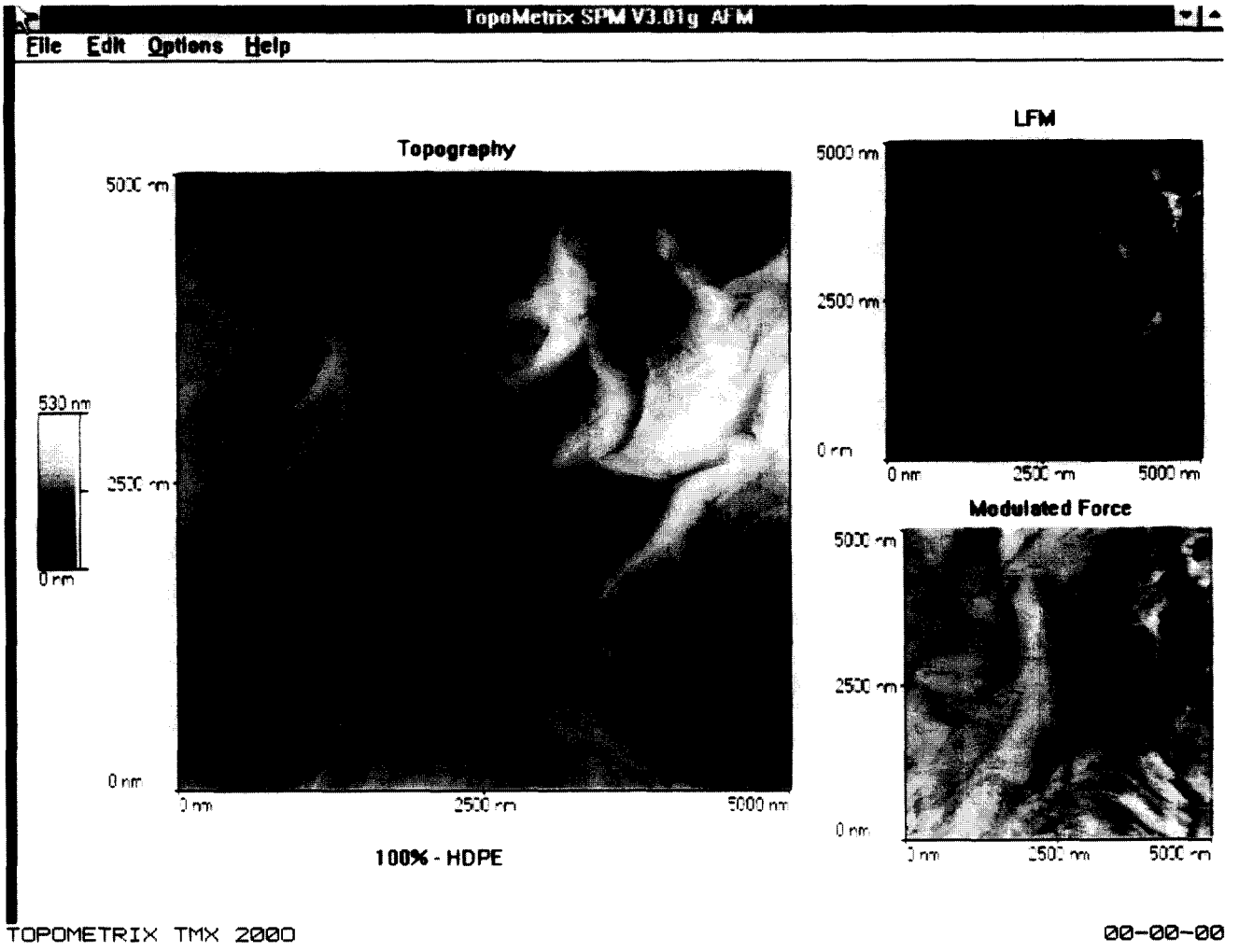

Figure 14 HDPE annealed surface AFM topographic, modulated force and lateral force images (5000 × 5000 nm)

$x = 0.96$, 0.96 and 0.58, respectively, and $d = 3.0$ Å, $x = 0.92$ for 20EAA using this model.

A second model was developed for the amorphous EVA co-polymer surfaces. This model is composed of three layers: a surface layer of ethylene, a middle layer of VA and a substrate of EVA (*Figure 18b*). The intensity of the C=OO signal from the middle VA layer is reduced by the top ethylene layer. Below these layers is bulk EVA. The intensity of the bulk signal is influenced by both of the top two layers. The predicted intensity of the C(1s) signal for the C=OO peak using this model is, using the ideas of Fulghum and Linton[35]:

$$I_o = I_o^\infty[1 - e^{-x/\lambda \cos\theta}]e^{-y/\lambda \cos\theta} + I_s^\infty e^{-(x+y)/\lambda \cos\theta} \quad (7)$$

where I_o is the intensity of the observed C=OO signal, I_o^∞ is the intensity of this signal from pure PVA, I_s^∞ is the signal intensity from the pure EVA co-polymer, x is the thickness of the VA layer and y is the thickness of the ethylene layer. Only the first term of the equation is needed for the 15° angle or approximately 15 Å penetration because the second term comes from the pure co-polymer base layer. This model fits the data within ± 12% for an ethylene layer thickness of 3 Å and a VA layer thickness of 6 Å for all the 70EVA samples.

CONCLUSIONS

1. Semi-crystalline EVA and EAA co-polymers with high wt% E (9EVA to 27.5EVA) had higher wt% VA at the surface than in the bulk, regardless of the type of sample preparation. Excess VA or AA at the surfaces of annealed semi-crystalline films was probably the result of the rejection of VA or AA units from the growing crystallites. Spin and solution cast films generally had a greater percentage of VA at their surfaces than annealed films; this additional excess may be caused by the lower solubility of the ethylene units in the toluene used for casting, leaving a layer of the more soluble VA units on the air surfaces.

2. Amorphous EVA co-polymers (50EVA and 70EVA) annealed films showed an excess of ethylene at the surface. This occurred even though there are only very short sequences of ethylene in these co-polymers and is probably caused by the lower surface free energy of the ethylene repeat units with respect to the VA repeat units.

3. The EAA co-polymers, all of which were semi-crystalline, always showed an excess of AA at the air surfaces. This occurred despite the much lower surface free energies of polyethylene *versus* PAA and was, like the excess of VA at the surfaces of the semi-crystalline EVA co-polymers, probably due to the rejection of the AA repeat units in these samples from the polyethylene crystallites.

4. The annealed surfaces of most of the 9EVA through 18EVA and 3EAA through 20EAA co-polymers had surface structures which appear to be spherulites in SEM micrographs. Topography mode AFM micrographs revealed similar surface structures in 9EVA and 18EVA, the spherulites having a radiating fibrous texture, with raised fibres.

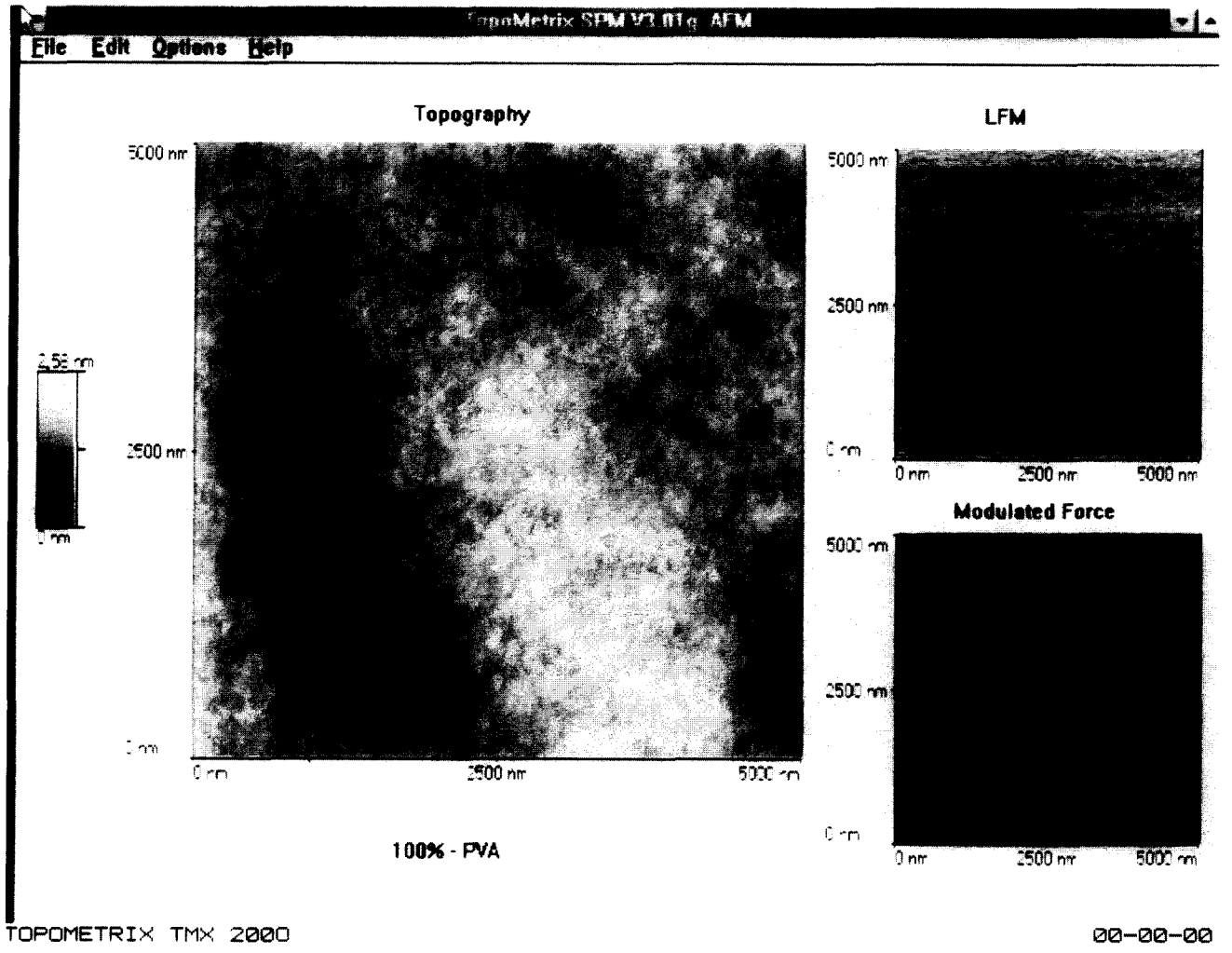

Figure 15 PVA annealed surface AFM topographic, modulated force and lateral force images (5000 × 5000 nm)

5. AFM bearing–ratio curves showed a fractional coverage of VA on 9EVA and 18EVA annealed surfaces of 0.885 and 0.927, respectively, by quantifying the amount of the 'harder' areas on the surfaces. Literature values of Shore hardness were used to determine that PVA is harder than polyethylene at room temperature. The XPS data were used with a simple model, which assumed a partial VA layer over a polyethylene layer at annealed co-polymer surfaces, to calculate a 2.0 Å layer of VA on the 9EVA and 18 EVA surfaces, with surface coverages of 0.91 and 0.96, respectively, in reasonable agreement with the AFM bearing–ratio data.

ACKNOWLEDGEMENTS

This research was supported in part by the Donors of the Petroleum Research Fund administered by the American Chemical Society and in part by the late Mr Alfred Horka. Thanks to the Rubber Division of the American Chemical Society, who provided one of us (R.L.M.) with the Paul Flory Memorial Fellowship in 1992–93 and 1993–94. Thanks also to Inga Green, Department of Biology, for help with the SEM, to James V. Crivello, Department of Chemistry, for the use of his d.s.c., to Ray Eby of Topometrix for providing the AFM data, and to Chan I. Chung, Department of Materials Engineering, for donation of some of the polymer samples.

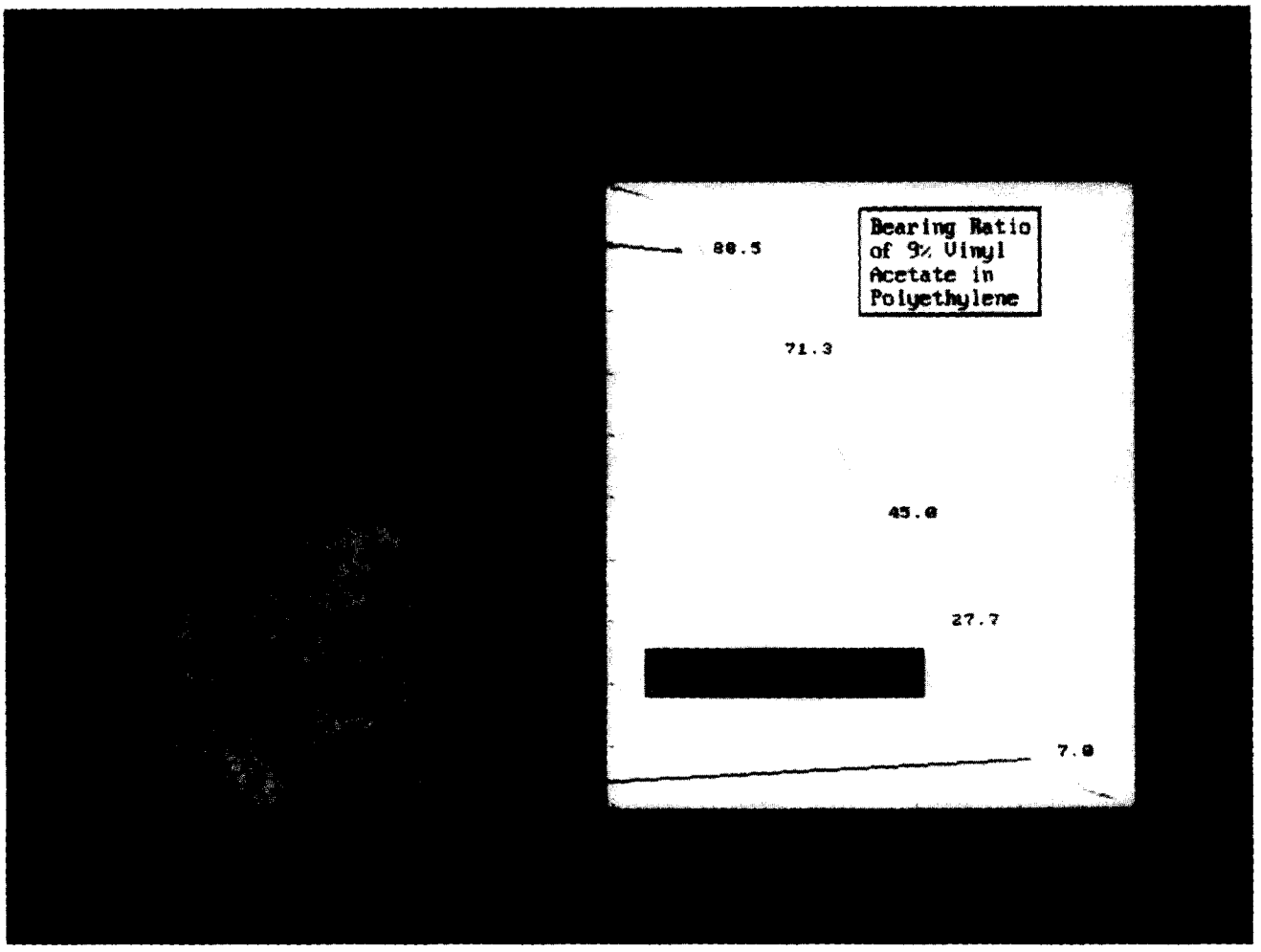

Figure 16 9EVA annealed surface AFM bearing–ratio curve from modulated force mode

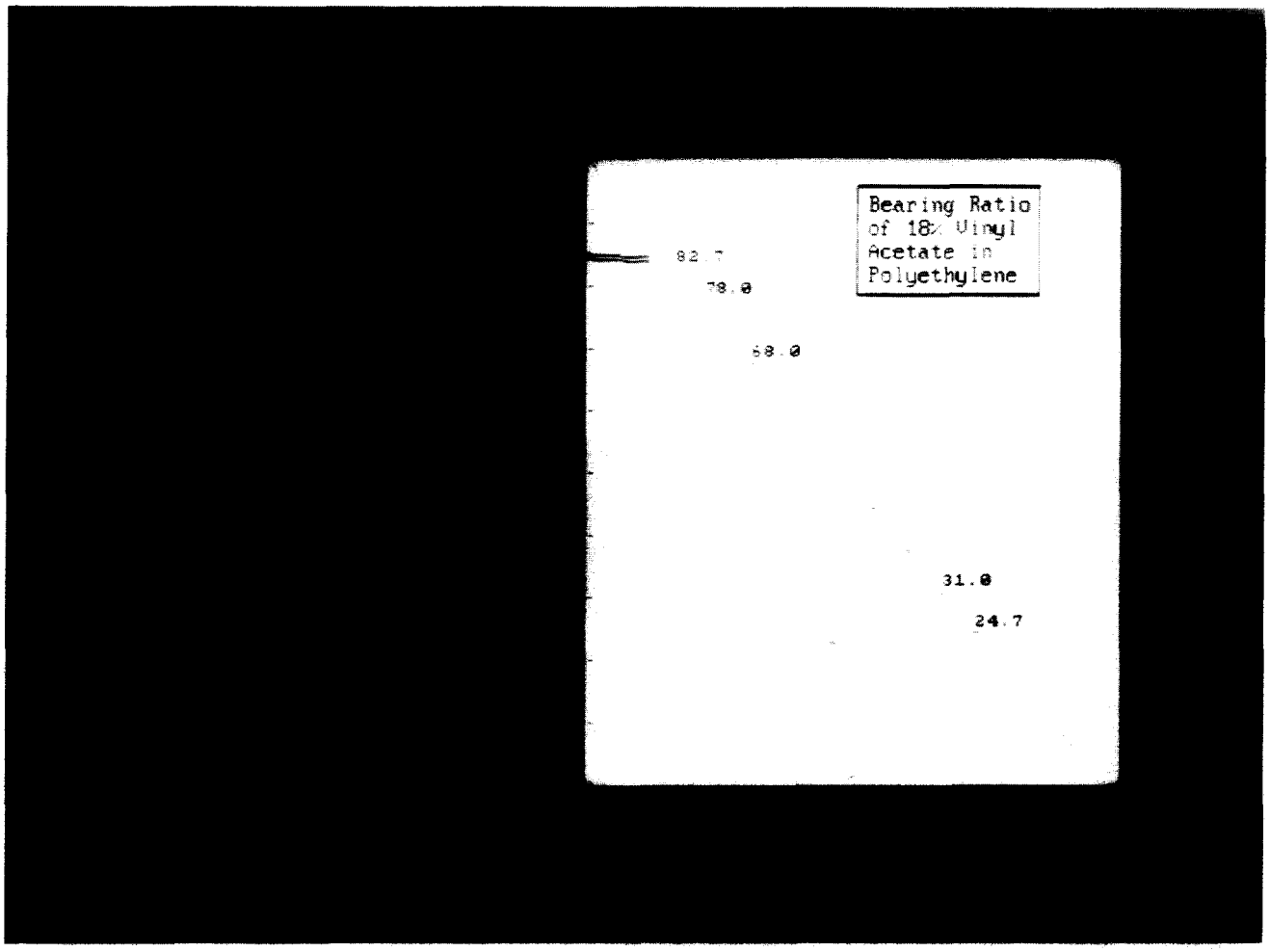

Figure 17 18EVA annealed surface AFM bearing–ratio curve from modulated force mode

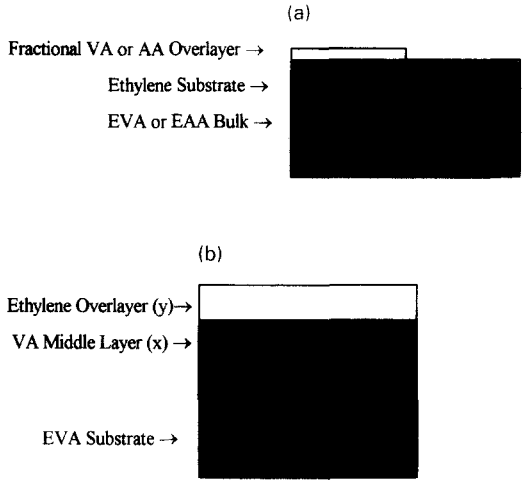

Figure 18 (a) Model of a fractional VA or AA overlayer over a pure ethylene layer on semi-crystalline co-polymer surfaces. (b) Model of a surface layer of ethylene, mid-layer of VA and substrate of EVA on amorphous co-polymer surfaces.

REFERENCES

1. Gaines, G. L. Jr and Bender, G. W., *Macromolecules*, 1972, **5**, 82.
2. Thomas, H. R. and O'Malley, J. J., *Macromolecules*, 1979, **12**, 323.
3. O'Malley, J. J., Thomas, H. R. and Lee, G. M., *Macromolecules*, 1979, **12**, 996.
4. Thomas, H. R. and O'Malley, J. J., *Macromolecules*, 1981, **14**, 1316.
5. Schmitt, R. L., Gardella, J. A. Jr, Magill, J. H., Salvati, L. Jr and Chin, R. L., *Macromolecules*, 1985, **18**, 2675.
6. Busscher, H. J., Hoogsteen, W., Dijkema, L., Sawatsky, G. A., van Pelt, A. W. J., de Jong, H. H. and Arends, J., *Polym. Commun.*, 1985, **26**, 252.
7. Tezuka, T., Fukushima, A., Matsui, S. and Imai, K., *J. Colloid Interface Sci.*, 1986, **114**, 16.
8. Schmitt, J. J., Gardella, J. A. Jr and Salvati, L. Jr, *Macromolecules*, 1989, **22**, 4489.
9. Li, W. and Huang, B., *Polym. Bull.*, 1988, **20**, 531.
10. Patel, N. M., Dwight, D. W., Hedrick, J. L., Webster, D. C. and McGrath, J. E., *Macromolecules*, 1988, **21**, 2689.
11. Yoon, S. C. and Ratner, B. D., *Macromolecules*, 1988, **21**, 2401.
12. Zhao, X., Zhao, W., Sokolov, J., Rafailovich, M. H., Schwarz, S. A., Wilkens, B. J., Jones, R. A.L. and Kramer, E. J., *Macromolecules*, 1991, **24**, 5991.
13. Bhatia, Q. S. and Burrell, M. C., *Polymer*, 1991, **32**, 1948.
14. Chen, X., Gardella, J. A. Jr, Ho, T. and Wynne, K. J., *Macromolecules*, 1995, **28**, 1635.
15. Blahovici, T. and Brown, G., *Polym. Eng. Sci.*, 1988, **28**, 1381.
16. Kumler, P., Matteson, H. and Gardella, J., *Langmuir*, 1991, **7**, 2479.
17. Affrossman, S., Hartshorne, M., Jerome, R., Munro, H., Pethrick, R. A., Petitjean, S. and Rei Vilar, M., *Macromolecules*, 1993, **26**, 5400.
18. Chihani, T., Bergmark, P. and Flodin, P., *J. Adhesion Sci. Technol.*, 1993, **7**, 327.
19. Galuska, A. A., *Surface Interface Anal.*, 1994, **21**, 703.
20. Chihani, T., Bergmark, P. and Flodin, R., *J. Adhesion Sci. Technol.*, 1995, **9**, 843.
21. Wunderlich, B. and Czornyj, G., *Macromolecules*, 1977, **10**, 906.
22. Briggs, D., in *Practical Surface Analysis*, Vol. 1, ed. D. Briggs and M. P. Seah. Wiley, New York, 1990.
23. Clark, D. T. and Thomas, D. T., *J. Polym. Sci., Polym. Chem. Ed.*, 1977, **15**, 2843.
24. Wu, T. K., Overnall, D. W. and Reddy, G. S., *J. Polym. Sci., Polym. Phys. Ed.*, 1974, **12**, 901.

25. Randall, J., *Polymer Sequence Determination*. Academic, New York, 1977.
26. Muilenberg (ed.), *Handbook of X-Ray Photoelectron Spectroscopy*. Perkin Elmer Corp., 1979.
27. Thomas, H. R. and O'Malley, J. J., *Macromolecules*, 1979, **12**, 323.
28. O'Malley, J. J., Thomas, H. and Lee, G., *Macromolecules*, 1979, **12**, 996.
29. Schmidt, J., Gardella, J. Jr and Salvati, L. Jr, *Macromolecules*, 1989, **22**, 4489.
30. Yoon, S. C. and Ratner, B., *Macromolecules*, 1988, **21**, 2401.
31. Alamo, R., Domszy, R. and Mandelkern, L., *J. Phys. Chem.*, 1984, **88**, 6587.
32. Domszy, R. C., Alamo, R., Mathiew, P. J. H. and Mandelkern, L., *J. Polym. Sci., Polym. Phys. Ed.*, 1984, **22**, 1727.
33. Danielas, W. E., in *Encyclopedia of Polymer Science Engineering*, Vol. 17, 2nd edn. Wiley, New York, 1989, p. 393.
34. Ritchie, P. D. (ed.), *Vinyl and Allied Polymers*. V.H.I., London, 1968.
35. Fulghum, J. E. and Linton, R. W., *Surface Interface Anal.*, 1988, **13**, 186.
36. Clark, D. T. and Thomas, H. R., *J. Polym. Sci. Polym. Chem. Ed.*, 1977, **15**, 2843.
37. Wu, S., *Polymer Interfaces and Adhesion*. Dekker, New York, 1982.
38. Bicerano, J., *Prediction of Polymer Properties*. Dekker, New York, 1993.